A northern boundary current along Australia's southern shelves: The Flinders Current

John F. Middleton and Mauro Cirano[1]

School of Mathematics, University of New South Wales, Sydney, New South Wales, Australia

Received 1 November 2000; revised 15 August 2001; accepted 23 August 2001; published 20 September 2002.

[1] South of Australia, the monthly mean wind stress curl is positive during both summer and winter and leads to Ekman pumping and downwelling throughout the region. Sverdrup dynamics indicates that this downwelling should lead to a northward transport of around 5–10 Sv (1 Sv = 10 m^3 s^{-1}). Classical arguments for western boundary currents are adapted to show that this transport should be deflected into an upwelling favorable boundary current that flows from east to west along Australia's southern shelves: the Flinders Current. Support for this proposition is obtained from results of the Ocean Circulation and Climate Advanced Modelling project (OCCAM), Sverdrup transports, and limited observations for the region. In addition, the OCCAM results show that the northward transport leads to upwelling at depths below 400 m and that the Flinders Current (1) intensifies from Victoria to Western Australia (transport ~8 Sv with speeds up to 15 cm s^{-1}), (2) can extend from the surface to depths of 800 m, and (3) is found during both summer and winter. During winter the winds are downwelling favorable and lead to a coastal current that flows from west to east and opposes the Flinders Current. Further support for the origin and nature of the Flinders Current is obtained from simple numerical experiments made using a rectangular domain and idealized representations of the summer and winter wind stress. *INDEX TERMS:* 4219 Oceanography: General: Continental shelf processes; 4279 Oceanography: General: Upwelling and convergences; 4532 Oceanography: Physical: General circulation; 4576 Oceanography: Physical: Western boundary currents; *KEYWORDS:* Boundary currents, ocean circulation, Sverdrup transport, Flinders Current

Citation: Middleton, J. F., and M. Cirano, A northern boundary current along Australia's southern shelves: The Flinders Current, *J. Geophys. Res.*, *107*(C9), 3129, doi:10.1029/2000JC000701, 2002.

1. Introduction

[2] Few modeling studies and even fewer observations have been made of the circulation along Australia's southern coastline, which faces an ocean subject to a positive wind stress curl and northward Sverdrup transport. The existence of this transport and its possible importance to the circulation along Australia's southern shelves were first noted in the analysis of *Bye* [1983], who used a rectangular analytical model and annual mean wind stress curl to show that a westward flowing boundary current should exist off the shelves south of Australia. Supporting evidence from hydrographic data was also given, and the flow was named the Flinders Current [*Bye*, 1972]. A northwestward transport for the region was also noted by *Godfrey* [1989] in a global analysis of Sverdrup transport, while limited observations [*Callahan*, 1972; *Hufford et al.*, 1997] show the existence of a westward flowing current along Australia's southern shelves. Indeed, *Hufford et al.* [1997] comment that the westward current might arise from the wind stress curl south of Australia, although no analysis was presented.

[3] Following *Bye* [1972], this westward flowing current will be called the Flinders Current and will be shown to be best characterized as a northern boundary current that results from the wind stress curl and Sverdrup dynamics. The current is quite distinct from other major current systems of the region. For example, the Leeuwin Current is a seasonal shelf break current that enters from the west, while the near-coastal currents are driven by surface Ekman transport and change direction with season.

[4] In section 2, evidence for the Flinders Current is obtained from the output of a global circulation model, and a comparison is made with the limited observations for the region. Ideas of western boundary circulation are adapted to explain the direction of the Flinders Current and associated deep upwelling. In section 3 the equatorward transports in the Ocean Circulation and Climate Advanced Modelling project (OCCAM) model will be shown to be dominated by the Sverdrup component that is driven by the curl of the wind stress. In section 4 an idealized numerical model is used to examine timescales of spin-up and to confirm that a northern boundary current (and associated upwelling) will exist during both

[1]Now at Centro de Pesquisa em Geofisica e Geologia, Instituto de Geociências, Universidade Federal da Bahia, Ondina, Brazil.

0148-0227/02/2000JC000701$09.00

summer and winter, even when the coastal currents reverse.

2. Results From the OCCAM Global Model and Sverdrup Dynamics

[5] Results for the summer and winter averaged wind stress fields (τ) are presented in Figures 1 and 2 [*Siefridt and Barnier*, 1993]. The monthly averages prepared by Siefridt and Barnier were also used to force the OCCAM global ocean model [*Webb et al.*, 1998]. The resultant seasonally averaged transport stream function is also presented.

[6] During both seasons the wind stress curl is positive ($\sim 10^{-7}$ Pa m^{-1}) and leads to downwelling favorable Ekman pumping throughout most of the region. Coastal winds have a magnitude of around 0.05 Pa but reverse between the two seasons, being upwelling and downwelling favorable during summer and winter.

[7] Features evident in the plot of the transport stream function during summer (Figure 1b) include the East Australian Current (southeast corner) and a general anticyclonic motion in the west that is associated with the anticyclonic forcing apparent in the wind stress. Of interest here is the generally equatorward transport found throughout the domain and the westward flow along the 4000-m isobath that begins near Portland in the east.

[8] Depth-integrated transports obtained from OCCAM and for the four sections shown in Figure 3 are presented in Table 1. For summer the transport through the zonal section closest to the shelf (36°S) is ~10 Sv. Much of this is deflected to the left through the meridional section at 122°E.

[9] Wintertime results for the stream function are presented in Figure 2b and also show the flow to be generally directed toward the north, although a boundary current is less evident and the transports are weaker than in summer. From Table 1 the northward transport at 36°S is ~4 Sv and again deflected into the westward flowing Flinders Current.

[10] The cross-shelf structure of the Flinders Current and associated density field are presented in Figure 4 for a westerly section (122°E) where the boundary current is largest. During winter (Figures 4a and 4b) the maximum westward speed is ~16 cm s^{-1} and occurs at a depth of 400 m. At and below this depth the isopycnals are upwelled, and the associated thermal wind shear acts to reduce the magnitude of the boundary current to near zero at a depth of 1200 m. Above 400 m the isopycnals are downwelled as a result of the wind forcing and cooling. Very light water is also found within 0.5° of the coast and at depths of 200 m or less. This water and the strong eastward currents (~30 cm s^{-1}) are associated with the Leeuwin Current. Observations [*Church et al.*, 1989] suggest that the current is stronger (up to 1 m s^{-1}) than the model would suggest, although the hydrographic structure is similar to that shown in Figure 4a. It also seems likely that the Flinders Current acts to feed the undercurrent of the Leeuwin Current observed farther to the north [*Church et al.*, 1989].

[11] The Leeuwin Current is absent during summer, although a weak eastward flowing current (~10 cm s^{-1}) is still found near the coast (Figure 4c). Atmospheric heating results in the development of an 80-m-deep stratified surface layer (Figure 4d), although the density field and Flinders Current are similar to that found during winter. Results farther to the east of those presented in Figure 4 are similar, although the maximum speed of the Flinders Current at 140°E is reduced to 4 and 6 cm s^{-1} during winter and summer, respectively.

[12] Before examining observations of the Flinders Current, we first present explanations for its direction and the notable upwelling of the deep thermocline. Both are adapted from classical arguments for the existence of western boundary currents and assume that the equatorward transport arises from Sverdrup dynamics.

[13] The first explanation involves the dissipation of vorticity. For midlatitude gyres the anticyclonic vorticity acquired by the equatorward Sverdrup transport can only be dissipated in a frictional western boundary layer, so that upon leaving this layer the total vorticity will match that of the surrounding fluid [*Gill*, 1982].

[14] A similar argument may be made here. Fluid columns will acquire anticyclonic vorticity as they move equatorward, and upon reaching the shelf the flow must be either to the west or to the east as shown in Figures 5a and 5b, respectively. In both cases the magnitude of the alongshore velocity should decrease offshore if only because the shelf depth increases with offshore distance. Bottom friction will act to reduce the magnitude of the current, and for the westward case (Figure 5a) this means the removal of anticyclonic vorticity that was acquired from the equatorward Sverdrup flow. As in the case of the western boundary current the vorticity of a column leaving the northern boundary current could then match that of the surrounding fluid. For the eastward flow (Figure 5b) this cannot happen as friction will act to decrease the cyclonic vorticity of the boundary current and increase the anticyclonic vorticity.

[15] A second explanation for the direction of the boundary current adapted from *Cushman-Roisin* [1994] involves the fate of the water that is downwelled at the surface by the wind stress curl. For a westward flowing boundary current the Ekman transport in the bottom boundary layer should decrease offshore as the overlying alongshore currents are weaker (Figure 5c) and should be upwelling favorable. As shown, this means that water must be drawn in from the interior so that upwelling occurs outside of the frictional bottom layer. Moreover, a steady state might be achieved since the water taken up in the bottom boundary layer can balance that downwelled at the surface by the wind stress curl. For an eastward flowing current the bottom boundary layer is downwelling favorable, and water will be expelled into the interior as shown in Figure 5d. No steady state is possible.

[16] We now turn to the observations of the Flinders Current and associated hydrography. *Callahan* [1972] used 2 days of current meter and summertime hydrographic data from a meridional section at 132°E to estimate zonal currents and transports. The results were qualitatively similar to those obtained from the hydrographic data and a near-bottom level of no motion, which indicate a westward transport of 8 Sv between 35°S and 39°S. The 10 Sv obtained from OCCAM (Figure 1b) for this section is in good agreement with this estimate. In addition, between 40°S and 45°S the transports estimated by *Callahan* [1972] become directed to the east and then west, a result that is again in agreement with the OCCAM results (Figure 1b).

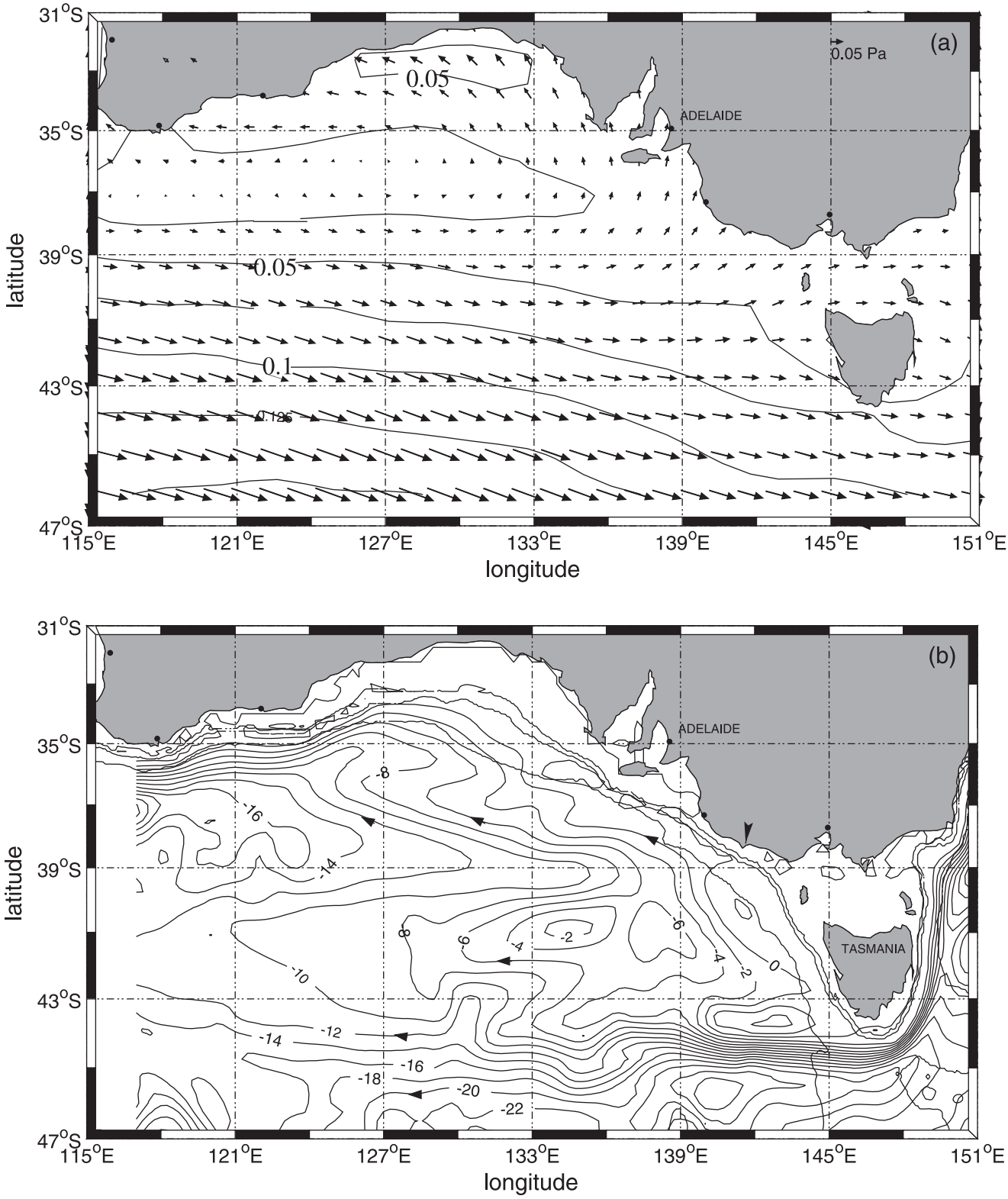

Figure 1. (a) Averaged surface wind stress for the Austral summer. The indicated vector has a magnitude of 0.05 Pa. The solid contours represent the magnitude of the wind stress. (b) Depth-integrated transport stream function obtained from the Austral summer-averaged OCCAM model results (units Sv). The direction of the flow is indicated by the arrows. The light lines represent the locations of the 200-, 1000-, and 4000-m isobaths.

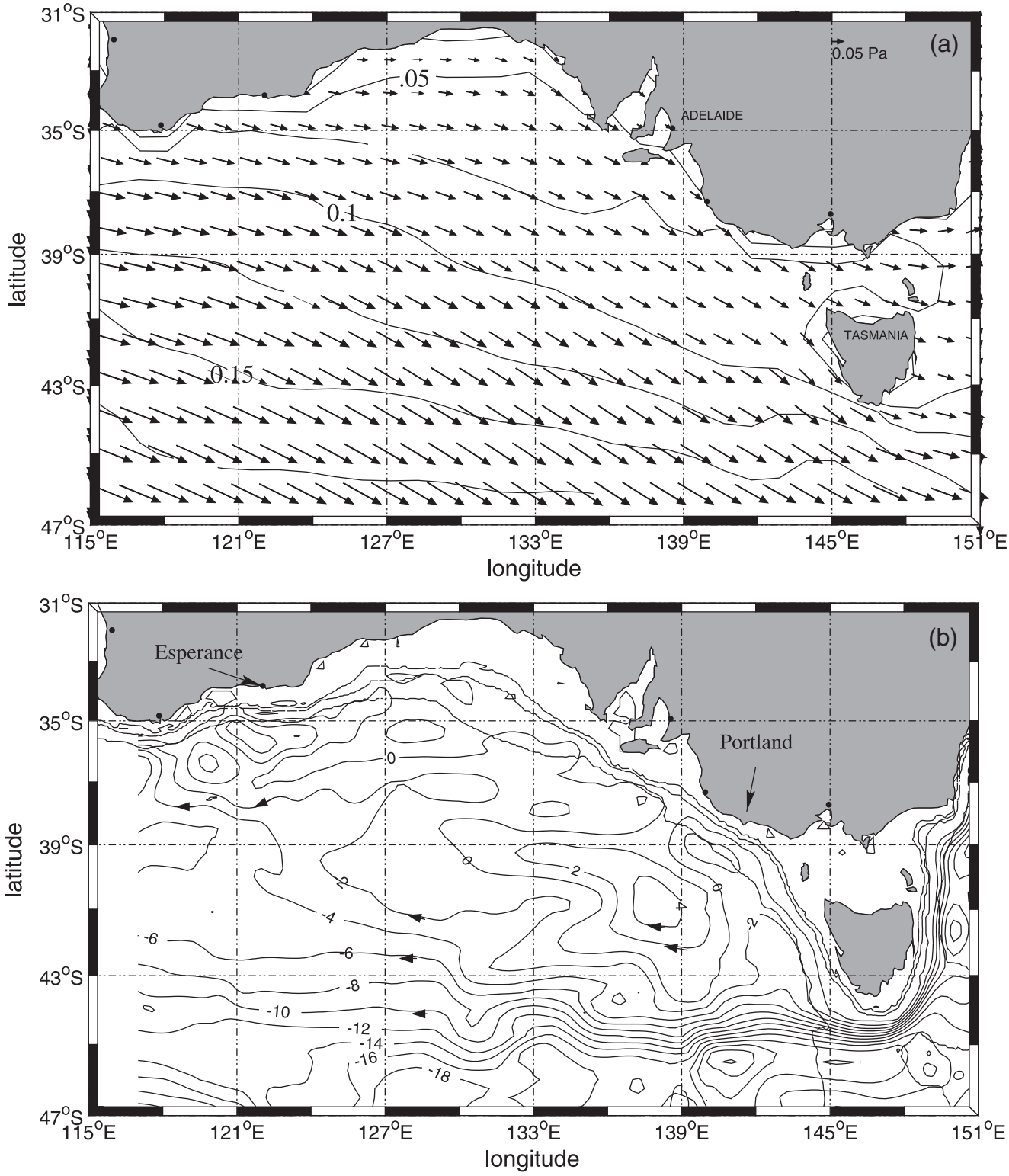

Figure 2. As in Figure 1 but for the wintertime results.

[17] More recently, *Schodlok and Tomczak* [1997a] used hydrographic data (November–December) in an inverse box model to infer the zonal transports through a 120°E section. They found the total transport to be dominated by that in the top 1200 m, with a net westward transport of 35 Sv between 39°S and the coast. This value is about twice the 16 Sv for the OCCAM model (Figure 1b), but the directions are the same. Using a level of no motion close to 2000 m, *Schodlok and Tomczak* [1997b] also found currents within 100 km of the coast and at 122°E to be directed to the west and to be largest at depths of order 500 m, a result that is not inconsistent with the westward maximum at 400 m shown in Figure 4.

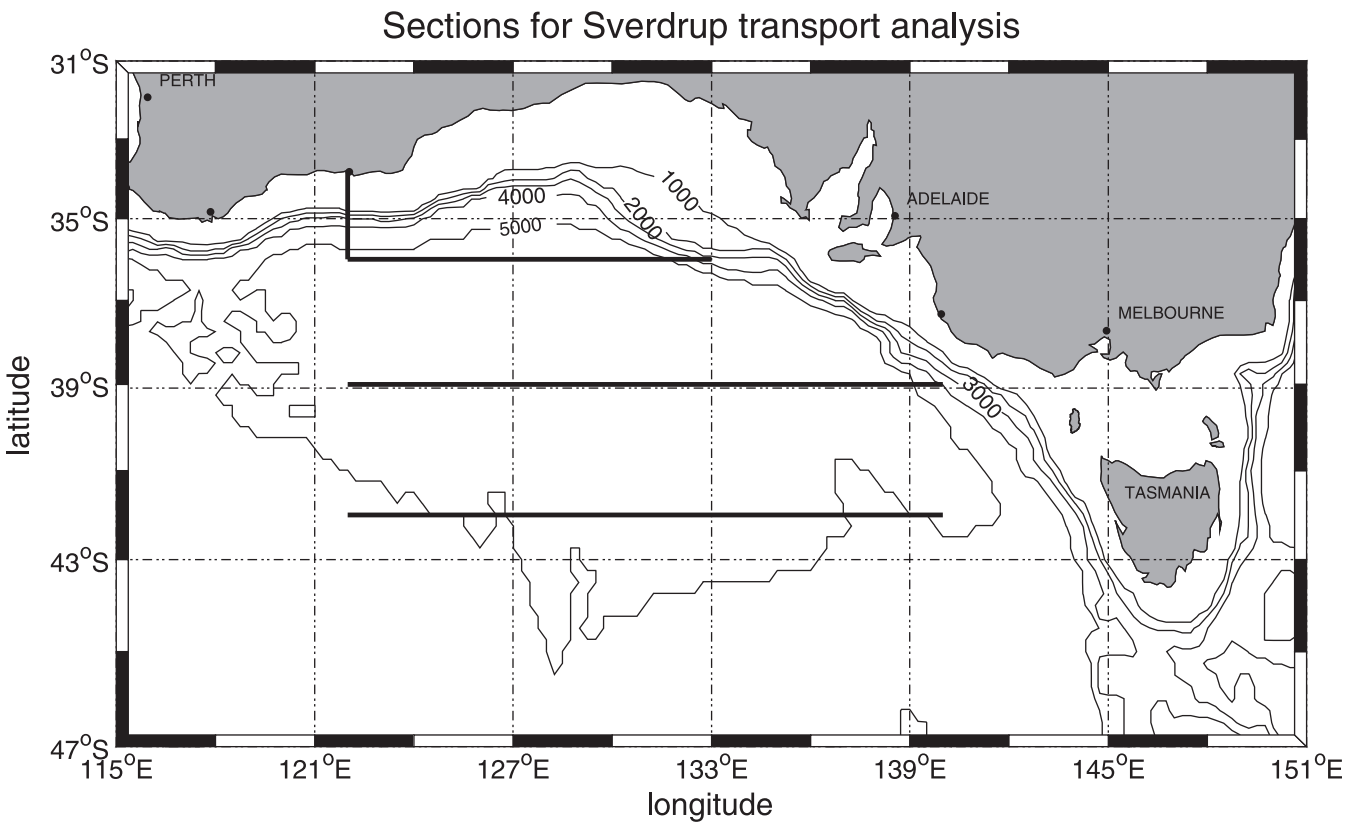

Figure 3. Topography of the region south of Australia. The 1000-, 2000-, 3000-, 4000-, and 5000-m isobaths are indicated. The solid lines correspond to the sections used to determine transports.

[18] The hydrographic data obtained by *Schodlok and Tomczak* [1997b] also show the deep thermocline (500–1000 m) to be upwelled toward the coast and over a distance of 100 km. Deep, strong upwelling is also apparent for all seasons in the Levitus data and to the west of 130°E: The OCCAM results suggest that the Flinders Current (and associated upwelling) intensify to the west, so these observations are consistent with the model output. As noted above, such upwelling is a necessary component of the northern boundary current.

[19] Summertime acoustic Doppler current profiler (ADCP) measurements were also obtained by *Hufford et al.* [1997] for the 115°E section. A depth of 1500 m was identified as an approximate level of no motion. Between the coast and 37°S the zonal transport above and below this level was estimated to be 22 Sv (westward) and 5 Sv (eastward), yielding a net of 17 Sv to the west. From Figure 1b the net OCCAM transport for this section is 16 Sv to the west and in very good agreement with the observations. Between 37°S and 40°S the transport above and below the 1500-m level was observed to be 12 Sv (eastward) and 5 Sv (westward), yielding a net 7 Sv to the east. The OCCAM results indicate a 10-Sv transport to the east.

[20] While some 13 other long-term current meter moorings have been maintained within the Bight region, only one was deployed either deep enough or far enough offshore to resolve the Flinders Current. That meter was deployed off the west coast of Tasmania (43°S) at a depth of 995 m (water depth 2000 m) by *Lyne and Thresher* [1994]. The wintertime average was found to be 4 cm s^{-1} to the north

Table 1. Net Transports[a]

Section	OCCAM	Sverdrup (Flat)	Sverdrup (Topographic)	Ekman
		Summertime		
41°S	5.0	10.7	8.3	1.2
39°S	13.5	11.9	11.0	0.6
36°S	9.7	8.8	−1.2	−0.1
122°E	−10.6	-	-	-
		Wintertime		
41°S	7.1	6.9	5.7	1.6
39°S	2.6	4.3	4.0	1.5
36°S	4.1	3.9	0.5	0.8
122°E	−4.8	-	-	-

[a]Net transports are in Sv. For zonal sections, positive values are to the north; for meridional section at 122°E, negative values are to the west.

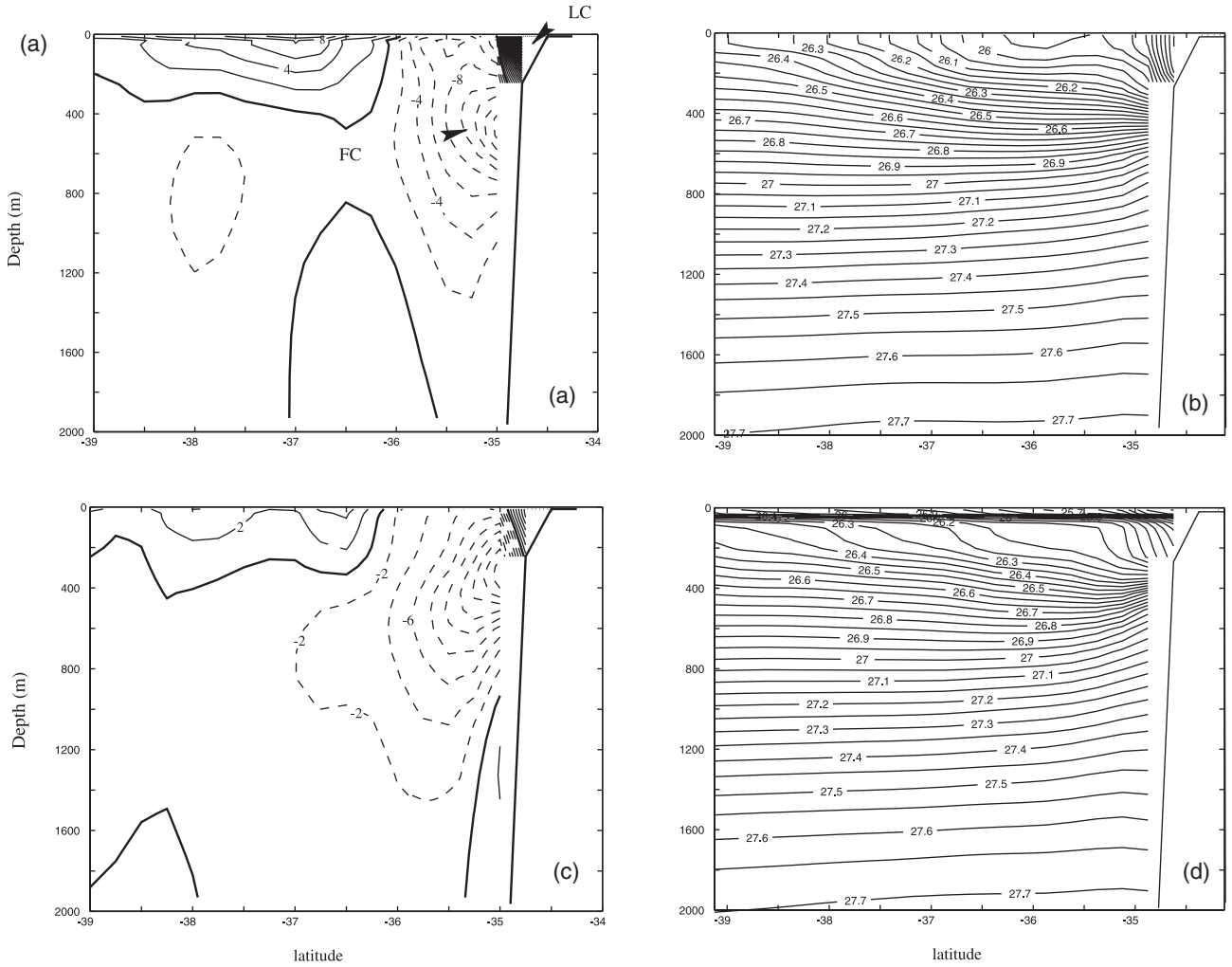

Figure 4. Cross-shelf results at 122°E from OCCAM. (a) The wintertime alongshore velocity (units cm s^{-1}). The Flinders Current (FC) and Leeuwin Current (LC) are labeled. The solid contours indicate eastward flow; dashed indicate westward. (b) The wintertime potential density field. (c) As in Figure 4a but for the summertime averages. (d) As in Figure 4b but for the summertime averages.

(M. Cirano and J. F. Middleton, The mean wintertime circulation along Australia's southern shelves: A numerical study, submitted to *Journal of Physical Oceanography*, 2002, hereinafter cited as Cirano and Middleton, submitted manuscript, 2002), while currents farther inshore or below depths of 200 m were found to be directed to the south. These results were found to be in good agreement with a high-resolution wintertime model of the region (Cirano and Middleton, submitted manuscript, 2002) and are also in crude agreement with the OCCAM results (not shown).

3. Sverdrup Transports and Spin-Up

[21] To determine the origin of the equatorward OCCAM transports, we consider two approximations for the Sverdrup transport. The first is for a barotropic, flat bottom ocean:

$$hv_F = k \cdot [\nabla \times \tau]/\beta\rho, \tag{1}$$

where k is the vertical unit vector, the x and y coordinates are directed to the east and north, β is taken to be 2.0×10^{-11} $(ms)^{-1}$, and the density ρ is constant.

[22] From Figure 3 it is clear that the ocean depth varies, and as a second approximation we will assume that the ocean depth h is a function only of the northward meridional coordinate y. This assumption is by no means exact so that the topographic transports obtained are only approximate. However, our purpose here is to determine the nature of the Sverdrup transports and show that they are an important component of those found in the OCCAM model and possibly the real ocean. Following *Thompson et al.* [1986], the topographic Sverdrup transport with $h=hy$ is

$$hv = V_E + fk \cdot [\nabla \times (\tau/f)]/\rho(\beta - \beta_T), \tag{2}$$

where $\beta_T = (f/h)dh/dy$ denotes the topographic vorticity gradient due to changes in ocean depth. The first term on the right side of equation (2) represents the meridional surface Ekman transport V_E. The second term on the right side of equation (2) represents the geostrophic flux associated with vortex squashing, and equation (2) may

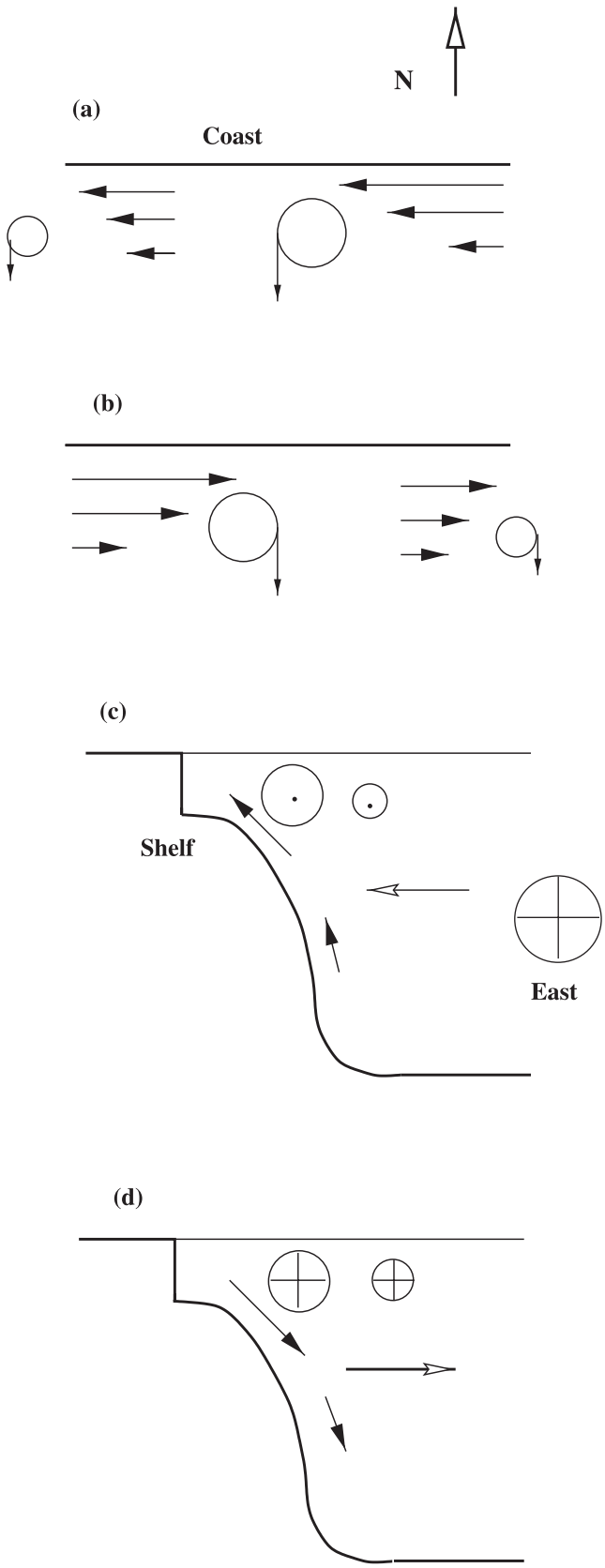

be rewritten in terms of the flat bottom Sverdrup transport (equation (1)) as

$$hv = -\beta_T V_E/(\beta - \beta_T) + \beta\, hv_F/(\beta - \beta_T). \quad (3)$$

[23] The Sverdrup transports given by equations (1) and (3) represent steady state solutions for a barotropic ocean that are set up by the zonal passage of Rossby waves across the oceanic domain. However, differences between these and the OCCAM transports can arise since the winds vary seasonally and a steady state Sverdrup balance might not be achieved. Stratification can also be important since thermal wind shear associated with the baroclinic modes can act to minimize near-bottom currents and reduce the influence of topographic variations on the depth-integrated Sverdrup transport [*Anderson and Killworth*, 1977]. As *Gill* [1982, p. 511] states, "the vertically integrated transport in stratified models is very similar to that found in flat bottom barotropic models."

[24] A simple examination of these effects can be made by considering the timescale that governs the adjustment to the steady Sverdrup solutions. For purely zonal winds the scale is given by

$$T_B = B/c \quad (4)$$

and corresponds to the time taken for a Rossby wave, group speed c, to propagate across the ocean basin, width B. For an eastward wind stress with a meridional wave number l and $\tau^x = \tau_0 \cos(ly)$, *Anderson and Gill* [1975] have shown that the steady Sverdrup solution is set up after the passage of the westward propagating Rossby waves. The group speed for the long barotropic waves is given by $c = \beta l^{-2}$ [*Gill*, 1982] and, in this case, $B = 2000$ km. From Figure 1a we take $l = 2\pi/2000$ km so that $c = 2.0$ m s^{-1} and $T_B = 12$ days. The scale here is short compared with the seasonal scale of 180 days so that a steady setup of the barotropic component of the Sverdrup transport might be expected.

[25] For the baroclinic modes the fastest speed is $c_I = \beta a^2$, where a denotes the internal deformation radius. These waves act to displace the thermocline, redistribute the Sverdrup transport with depth, and make the near-bottom currents small. For the OCCAM model, a is ~30–60 km; the speed c_I is small, ~1.5–3.0 cm s^{-1}; and the baroclinic timescale T_B is large, ~2–4 years.

Figure 5. (opposite) A schematic illustration of the reasons for the westward flow of the northern boundary current (the Flinders Current) in the Southern Hemisphere. For Figures 5a and 5b, north is indicated by the arrow labeled "north," and the plan view shows currents trapped against a shelf and coast. (a) Anticyclonic vorticity (the arrowed circles) of a westward current (the arrows) trapped against the shelf. (b) As in Figure 5a but for an eastward current. (c and d) Cross sections of Figures 5a and 5b, respectively. The directions of the bottom Ekman transport are indicated by the solid arrows. The westward and eastward currents are indicated by the arrowheads and tails in Figures 5c and 5d, respectively. The direction east is indicated by the arrow tail labeled "east."

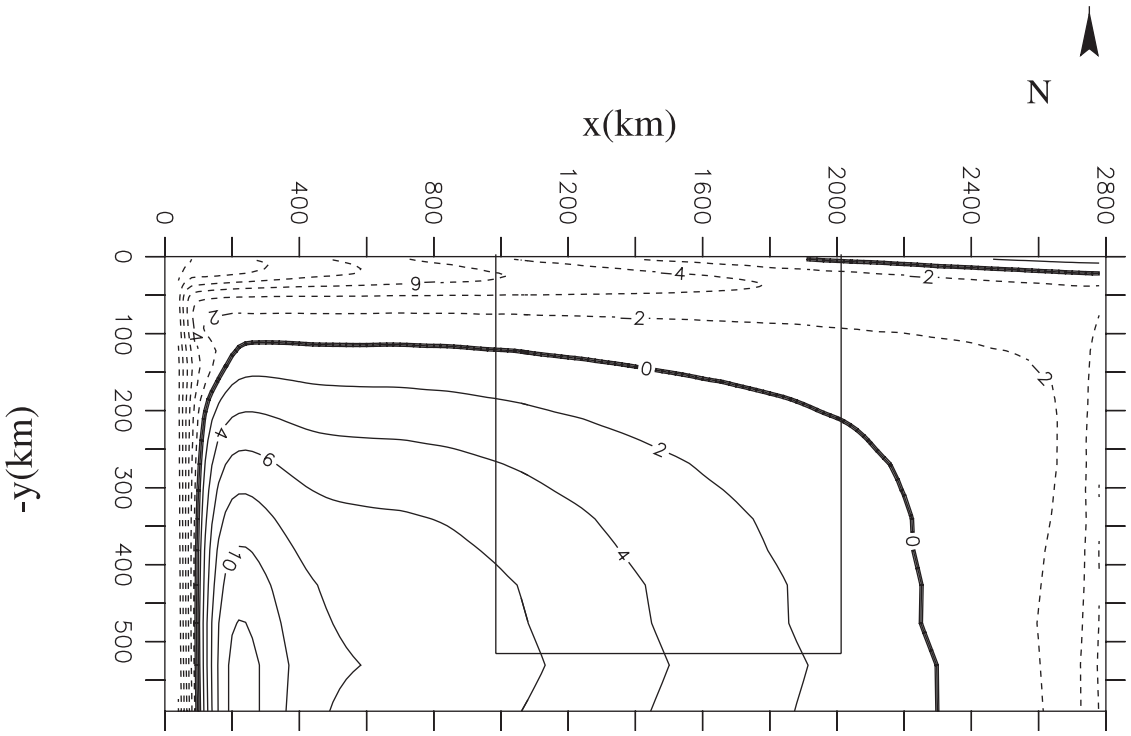

Figure 6. The sea level field (units cm) at day 30 and for the idealized numerical model and winter wind stress. Solid contours indicate positive displacement; dashed indicate negative. The sections for the transport calculations are indicated by the heavy solid lines and north (N) is indicated by the arrow.

[26] However, the seasonal change in the zonal component of the wind stress south of 41°S is not large, so a quasi-steady adjustment may be achieved by the baroclinic modes. For this region the effects of topographic slope would be minimized and the transports should be better described using that for a barotropic, flat bottom ocean (equation (1)).

[27] Now consider the net transports shown in Table 1. For each of the three zonal sections shown in Figure 3 the local value of the slope dh/dy, β_T, Ekman, and flat bottom Sverdrup transports were obtained, substituted into equation (3), and then integrated to determine the net topographic transport.

[28] At 41°S the ocean depth increases with y as shown in Figure 3. Thus since f is negative, $\beta_T = (f/h)dh/dy$ is negative, and the average value is -1.9×10^{-11} $(\text{ms})^{-1}$. From equation (2) the effective meridional gradient in planetary vorticity β-β_T is therefore larger, the beta effect is enhanced, and the Sverdrup transport is reduced by 20% or so from the flat bottom values shown in Table 1. The transport is reduced since for a given wind stress curl the change in latitude and velocity experienced by a fluid column is smaller because of the larger gradient of planetary vorticity β-β_T.

[29] As noted, the zonal component of wind changes little between seasons at 41°S, so adjustment by the baroclinic modes should be achieved and the OCCAM transports better estimated by the flat bottom Sverdrup transport (equation (1)). From Table 1 this is only true for winter; the summertime values are better estimated by the topographic transport (equation (3)). However, all of the transports are of comparable magnitude (5–10 Sv), indicating that Sverdrup dynamics drive a substantial component of the northward flow found in OCCAM at 41°S.

[30] Now consider the results at 39°S, which lies in the middle of a large topographic "bowl" bounded by the 5000-m isobath (Figure 3). The topographic slope is not large, and indeed, both the flat bottom and topographic Sverdrup transports are similar to those obtained from OCCAM, and both show a strong seasonal variation between summer (12 Sv) and winter (4 Sv).

[31] At the northernmost section (36°S) the winds reverse between the seasons, so baroclinic adjustment based on Rossby wave propagation is precluded and the barotropic Sverdrup transport should be given by the topographic expression (equation (3)). Indeed, the strong topographic slope ($dh/dy \sim -10^{-2}$) dominates the barotropic Sverdrup dynamics with the average sectional value of β_T being 18×10^{-11} $(\text{ms})^{-1}$ and much larger than β. During summer the Sverdrup transport is directed to the south, while during winter the net transport is weak and less than the onshore Ekman transport. That is, the geostrophic transport is directed to the south.

[32] Surprisingly, the flat bottom estimates at 36°S are in much closer agreement with those obtained from OCCAM (the topographic Sverdrup transports are less than one eighth of the OCCAM values). The reason for this is that baroclinic effects are again important but now arise from the presence of the shelf rather than Rossby wave propagation.

[33] To see this, consider first the cross-sectional results at 122°E shown in Figure 4. Below 400 m, seasonal variations of the density field are very small, and significant

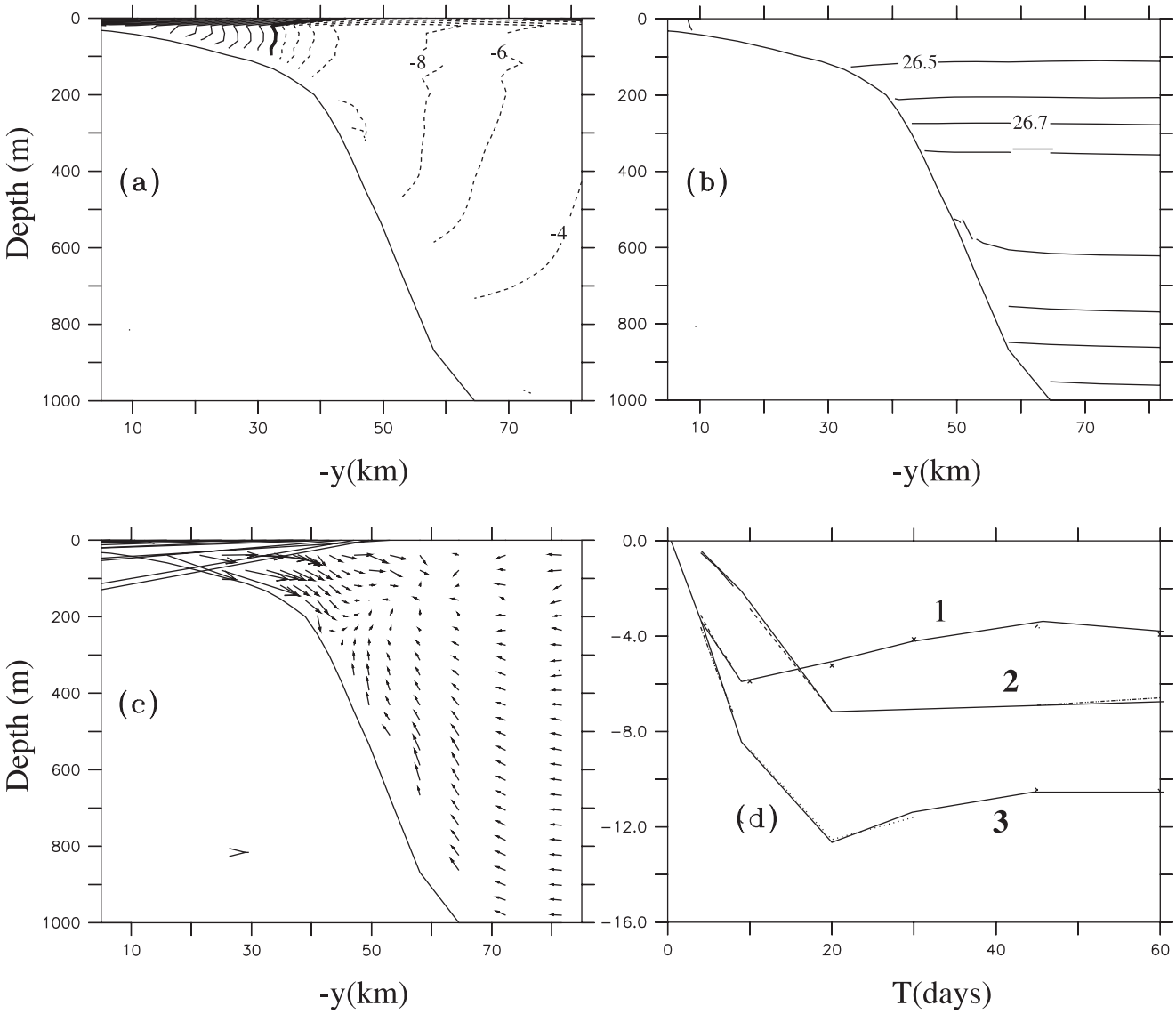

Figure 7. Cross-shelf results at x = 1500 km and at day 30 for the idealized model and winter wind stress. (a) The alongshore velocity (units cm s^{-1}, contour interval 2 cm s^{-1}). Solid contours indicate flow to the east; dashed indicate flow to the west. (b) Potential density field. (c) Cross-shelf velocity field (u, 100 w). The vector indicated has an amplitude of 0.5 cm s^{-1}. (d) Integrated net transports (units Sv) as a function of time for the winter forcing. Results are presented for the eastern section (curve 1), the southern section (curve 2), and the western section (curve 3).

upwelling occurs so as to take up water downwelled elsewhere at the surface by Ekman pumping. The resultant thermal wind shear leads to a decrease in the magnitude of the Flinders Current with depth, so the effects of bottom slope are small. A similar result pertains to the northward currents at 36°S. Below 400 m, the density field changes very little with season, and the isopycnals slope up toward the east, leading to the minimization of near-bottom northward currents and thus topographic effects.

4. Results of an Idealized Model

[34] To further examine the spin-up to the Sverdrup solution and resultant boundary current, results were obtained using the Princeton ocean model [*Blumberg and Mellor*, 1987] for an idealized wind stress curl and rectangular box topography (Figure 6). The zonal and meridional extent of the ocean basin was chosen to be 2800 and 1000 km, respectively, so as to crudely mimic the geometry of the Bight region. For simplicity, vertical walls were adopted on all boundaries except the northern zonal boundary where a 60-km-wide shelf was assumed (see Figure 7). The maximum water depth was 1000 m. Typical wintertime and summertime profiles for density were obtained at one point and adopted for the entire domain, so initially, horizontal variations in density do not exist. Further details of the model are presented by *Middleton and Cirano* [1999].

[35] For the region here, the parameter values $\beta = 2.0 \times 10^{-11}$ $(ms)^{-1}$ and $f = -0.83 \times 10^{-4}$ s^{-1} were adopted, and a zonal wind stress is prescribed by $\tau^x = \tau_0 + |y|\ \partial\tau^x/\partial y$,

where $|y|$ denotes the distance offshore from the northern coast. For both seasons we take $\partial\tau^x/\partial y$ to be constant and equal to 10^{-7} Pa m^{-1}, while for winter and summer we take $\tau_0 = 0.05$ Pa and -0.05 Pa, respectively. Wind at the coast is therefore upwelling and downwelling favorable during summer and winter.

[36] Results for sea level at day 30 and using the winter forcing are presented in Figure 6. The convergence of the onshore Ekman transport leads to Ekman pumping, which acts to raise sea level over the center of the domain. Since the flow is enclosed in a box, sea level generally falls on the outer edge of the central high. However, because of the northward Ekman transport sea level is raised along the northern coast and for x > 1900 km.

[37] An eastward current of up to 16 cm s^{-1} is established over the inner shelf as shown in the cross-shelf section in Figure 7a. Farther offshore the flow is westward as found in the OCCAM results and geostrophically consistent with the high-pressure pattern shown in the sea level results (Figure 6). An onshore flow associated with the northward Sverdrup transport is also evident (Figure 7c) and leads to upwelling and the raising of density surfaces at depths below 300 m or so (Figure 7b). While the upwelling does not appear to be strong at day 30, the thermal wind reduction in alongshore currents is apparent in Figure 7a. The results obtained using the summertime wind stress field are similar to those above except that the Ekman transport along the northern coast is upwelling favorable and leads to a westward current that is in the same direction as the boundary current found in deep water.

[38] The spin-up of the circulation is also of interest. In agreement with the analysis of *Anderson and Gill* [1975] phase plots (not presented) of the equatorward velocity obtained at (x, z) = (400 km, 250 m) indicate a linear growth in time due to the passage of the barotropic Rossby wave crest, with a speed estimated at $\sim$1.8 m s^{-1}. The value here is very close to that estimated above using Rossby wave dynamics, where $c = \beta\, l^{-2} \sim 2.0$ m s^{-1}. By day 16 the wave crest has reached the western boundary. By day 30 the barotropic circulation is quasi-steady throughout much of the deep ocean domain.

[39] This estimate of the barotropic spin-up time is supported by the estimates of the onshore net transport (Figure 7d) through the zonal section (2) shown in Figure 6. The transport reaches a maximum of $\sim$7.5 Sv at day 30 and then slowly drops to a value of 6.5 Sv by day 60. Of this, 0.6 Sv is due to the surface Ekman layer, leaving a total of 5.9 Sv that compares well with the value of 6.25 Sv predicted by the steady state Sverdrup balance (equation (1)).

[40] The baroclinic adjustment of the circulation away from the shelf occurs on a much larger timescale than the 30 days for the barotropic component. With an internal deformation radius $a \sim 10$ km, the speed of the fastest baroclinic mode is very small ($c_I \sim 0.2$ cm s^{-1}), and the timescale for spin-up is on the order of 30 years. The open ocean circulation of the model here is unrealistically barotropic compared with the OCCAM results since the latter model is initialized with Levitus data (already spun up) and run for 12 years.

[41] The alongshore transports shown in Figure 7d also become quasi-steady after 30 days or so. At day 60 the 4 Sv entering the easternmost section, 1, is augmented by the onshore Sverdrup transport, and a net 10.5 Sv leaves the westernmost section, 3, (very similar results were obtained using the summer wind forcing). For winter the net transport of water associated solely with the eastward flowing coastal current was determined. At the western and eastern sections the transport was equal to 0.4 and 1.0 Sv, respectively, the difference or divergence of 0.6 Sv being exactly equal to that supplied by the net onshore Ekman transport of the wind.

[42] The alongshore barotropic transports are quasi-steady after 30 days since the currents here result directly from the onshore barotropic component of the Sverdrup transport, which is simply deflected to the west by the shelf. The spin-up of the baroclinic component of the westward currents over the shelf will proceed more slowly since it is governed by advective processes that lead to the upwelling and thermal wind shear. The thermal wind shear reduces the magnitude of the northern boundary current near the bottom (Figure 7a) and redistributes the alongshore transport with depth. However, the depth-integrated transports are quasi-steady, as shown in Figure 7d.

5. Summary and Discussion

[43] The proposition examined here was that the positive wind stress curl over the ocean south of Australia would give rise to an equatorward (Sverdrup) transport that would in turn be deflected to the left leading to a westward flowing northern boundary current. A westward rather than eastward current should result so as to satisfy classical arguments for vorticity dissipation and mass conservation that were here adapted for a northern boundary current.

[44] Few studies and observations have been made for the region, and we have appealed to results from the OCCAM global model, which provide strong support for the above proposition. An upwelling favorable western boundary current was found in the OCCAM results ($\sim$5–10 Sv), with speeds of up to 16 cm s^{-1} off the shelves south of Australia and identified to be the Flinders Current. While the wind stress curl is positive for both seasons, the coastal winds are upwelling and downwelling favorable during summer and winter, leading to westward and eastward currents near the coast ($\sim$1 Sv) that reinforce or oppose the Flinders Current. Similar results were found using an idealized numerical model.

[45] For the OCCAM model the net northward transports were found to be best estimated by flat bottom Sverdrup dynamics, although the reason for this differs at each of the zonal sections examined. Poleward of 41°S, changes in the seasonal zonal component of wind stress are not large, so the baroclinic component of the Sverdrup transport is likely to be in a state of quasi-adjustment and near-bottom currents and topographic effects minimized. The resultant flat bottom Sverdrup transports ($\sim$5–10 Sv) were found to be similar to the northward transports estimated from OCCAM. (Timescales for adjustment to the barotropic component of the Sverdrup transport were short ($\sim$12 days).)

[46] At 39°S the topography is reasonably flat, and estimates of the topographic and flat bottom Sverdrup transports were found to be in good agreement with those

computed for both winter (4 Sv) and summer (∼13 Sv) from OCCAM. At 36°S the winds change direction with season, so a quasi-steady setup by Rossby wave propagation might not be achieved and the transports might be better described by topographic Sverdrup dynamics. Indeed, the topographic slope dominates the barotropic Sverdrup dynamics at this section, which predict a transport of −1.2 Sv to the south during summer. However, the transports for OCCAM were again found to be directed to the north during both summer (∼10 Sv) and winter (∼4 Sv) and well predicted by the flat bottom Sverdrup transport relation. The reason for this arises from the isopycnals, which slope up toward the shelf and toward the east. The thermal wind shear associated with these slopes in turn acts to minimize near-bottom currents and the effects of topographic slope.

[47] In general agreement with the above, numerical results obtained using an idealized rectangular geometry and forcing demonstrate a rapid (15–30 day) Rossby wave spin-up of the barotropic equatorward Sverdrup transport. Moreover, an upwelling favorable northern boundary current is also found that flows to the west during both summer and winter when coastal winds and currents reverse.

[48] Limited observations for the region provide support for the existence of the Flinders Current and results from OCCAM. Snapshots of hydrography and currents along 132°E [*Callahan*, 1972] and 115°E [*Hufford et al.*, 1997] indicate a westward transport between 35°S and 37°S of 8 and 17 Sv, respectively. These observations compare well with the OCCAM values of 10 and 16 Sv for the same sections. The inverse box model of *Schodlok and Tomczak* [1997a] predicts a westward transport of 35 Sv, although this is twice that obtained from the OCCAM model.

[49] Current meter records obtained at a depth of 995 m off the west Tasmanian shelf (water depth 2050 m) show that a mean northwestward current (∼4 cm s^{-1}) exists during winter (Cirano and Middleton, submitted manuscript, 2002). Density data obtained for the South Australian region also show a westward flowing current relative to the 2000 dB level [*Bye*, 1983]. The data of *Levitus and Boyer* [1994] also show that isopycnals tend to be upwelled toward the shelves south of Australia.

[50] Finally, the existence of the onshore Sverdrup transport may have important implications for the shelf/slope circulation for the region. As shown in Figure 7c, during winter the offshore transport over the shelf will converge with the onshore Sverdrup transport and may lead to the detachment of bottom boundary layer water and sediments into the interior. Similarly, during summer, results obtained elsewhere (J. F. Middleton and G. Platov, The summertime circulation along Australia's southern shelves: A numerical study, submitted to *Journal of Physical Oceanography*, 2002) show that the offshore Ekman and topographic Sverdrup transport within the Great Australian Bight converge with the onshore deep ocean Sverdrup transport. This convergence leads to a ridge in sea level and eastward current over the 300-m isobath, which extends from Esperance in the west to the shelves south of Adelaide (Figure 2). This eastward current opposes the westward currents found farther inshore and offshore. Eastward and westward currents are thus found during both summer and winter, and their importance to the transport of sediments and marine biota remains to be determined.

[51] **Acknowledgments.** Mauro Cirano was funded by a Brazilian CNPq Ph.D. scholarship, and this work was supported by Australian Research Council Grant A39700800. We thank Stuart Godfrey for suggesting that we examine the Sverdrup transport for the region, David Webb and the OCCAM group for making their model output freely available to us, and Allen Blumberg and George Mellor for making the Princeton model freely available.

References

Anderson, D. L. T., and A. E. Gill, Spin-up of a stratified ocean, with applications to upwelling, *Deep Sea Res. Oceanogr. Abstr.*, *22*, 583–596, 1975.

Anderson, D. L. T., and P. D. Killworth, Spin-up of a stratified ocean with topography, *Deep Sea Res.*, *24*, 709–732, 1977.

Blumberg, A. F., and G. L. Mellor, A description of a three-dimensional coastal circulation model, in *Three-Dimensional Coastal Ocean Models, Coastal Estuarine Sci. Ser.*, vol. 4, edited by N. S. Heaps, pp. 1–16, AGU, Washington, D.C., 1987.

Bye, J. A. T., Ocean circulation south of Australia, in *Antarctic Oceanology I, The Australian-New Zealand Sector, Antarctic Res. Ser.*, vol. 19, edited by D. E. Hayes, pp. 95–100, AGU, Washington, 1972.

Bye, J. T., The general circulation in a dissipative basin with longshore wind stresses, *J. Phys. Oceanogr.*, *13*, 1553–1563, 1983.

Callahan, J. E., Velocity structure and flux of the Antarctic Circumpolar Current south of Australia, *J. Phys. Oceanogr.*, *76*, 5859–5864, 1972.

Church, J. A., G. R. Cresswell, and J. S. Godfrey, The Leeuwin Current, in *Poleward Flows Along Eastern Ocean Boundaries, Coastal Estuarine Stud. Ser.*, vol. 34, edited by S. J. Neshyba, C. N. K. Mooers, and R. L. Smith, pp. 230–254, Springer-Verlag, New York, 1989.

Cushman-Roisin, B., *Introduction to Geophysical Fluid Dynamics*, Prentice Hall, Old Tappan, N. J., 1994.

Gill, A. E., *Atmosphere-Ocean Dynamics*, Academic, San Diego, Calif., 1982.

Godfrey, J. S., A Sverdrup model of the depth-integrated flow for the world ocean allowing for island circulations, *Geophys. Astrophys. Fluid Dyn.*, *45*, 89–112, 1989.

Hufford, G. E., M. S. McCartney, and K. A. Donohue, Northern boundary currents and adjacent recirculations off southwestern Australia, *Geophys. Res. Lett.*, *24*, 2797–2800, 1997.

Levitus, S., and T. P. Boyer, Temperature, in *World Ocean Atlas 1994*, vol. 4, *NOAA Atlas NESDIS*, 117 pp., U.S. Dep. of Commer., Washington, D.C., 1994.

Lyne, V. D., and R. E. Thresher, Dispersal and advection of macruronus novaezealandie (Gadiformes: Merlucciidae) larvae off Tasmania: Simulation of the effects of physical forcing on larval distribution, in *The Biophysics of Marine Larval Dispersal*, vol. 45, *Coastal and Estuarine Studies*, edited by P. W. Sammarco and M. L. Heron, pp. 109–136, AGU, Washington, D.C., 1994.

Middleton, J. F., and M. Cirano, Wind-forced downwelling slope currents: A numerical study, *J. Phys. Oceanogr.*, *29*, 1723–1742, 1999.

Schodlok, M. P., and M. Tomczak, The circulation south of Australia derived from an inverse model, *Geophys. Res. Lett.*, *24*, 2781–2784, 1997a.

Schodlok, M. P., and M. Tomczak, Deep sections through the South Australian Basin and across the Australian-Antarctic Discordance, *Geophys. Res. Lett.*, *24*, 2781–2784, 1997b.

Siefridt, L., and B. Barnier, Banque de Donness AVISO Vent/Flux: Climatologie des Analyses de Surface du CEPMMT, *Tech. Rep. 91-1430-025*, 43 pp., Inst. Fr. de Rech. pour l'Exploit. de la Mer, Brest, France, 1993.

Thompson, K. R., J. R. N. Lazier, and B. Taylor, Wind-forced changes in the Labrador Current Transport, *J. Geophys. Res.*, *91*, 14,261–14,268, 1986.

Webb, D., B. A. de Cuevas, and A. C. Coward, The first main run of the OCCAM global ocean model, *Tech. Rep. 34*, 43 pp., Southhampton Oceanogr. Cent., Southampton, UK, 1998.

M. Cirano, CPGG, Instituto de Geociências, Universidade Federal da Bahia, Campus Ondina, Salvador, Bahia 40170-290, Brazil. (mauro@cpgg.ufba.br)

J. F. Middleton, School of Mathematics, University of New South Wales, Sydney 2052, New South Wales, Australia. (john.middleton@unsw.edu.au)